972434

Development and Chamber Testing of Laser-Based Gas Sensors

Konstantin P. Petrov, Yasuharu Mine, Thomas Töpfer, Robert F. Curl, and Frank K. Tittel
Rice Univ.

John Graf
Lyndon B. Johnson Space Center

ABSTRACT

Recent advances in semiconductor lasers and nonlinear optical materials permit construction of compact sensors that can measure trace air contaminants with high precision in real time, without sampling. A portable prototype sensor was built and tested in laboratory and field environments. This spectroscopic instrument measures carbon monoxide (CO) at concentrations between 0.1 and 10 ppm in air with 0.001 ppm precision, and 10-second response time. It uses 4.6-μm difference-frequency generation in periodically-poled lithium niobate (PPLN), pumped by two compact solid-state lasers. The sensor was used to measure the CO concentration profiles in chamber air during the Lunar-Mars Life Support Test Project (LMLSTP) Phase IIA test at NASA JSC. It is proposed to modify the instrument to measure several gases simultaneously, including formaldehyde. Projected use of fiber-coupled diode lasers and waveguide PPLN will permit development of a commercially viable, field-ready instrument.

INTRODUCTION

Safe use of human spacecraft requires detection, measurement, and removal of trace air contaminants such as carbon monoxide (CO), formaldehyde (H_2CO), ammonia (NH_3), hydrazine (N_2H_4), and hydrocarbons. Detection of these and other gases presently involves different techniques, most of which are gas-specific. Carbon monoxide, for example, can be measured with electrochemical sensors[1], gas tubes[2], and non-dispersive infrared analyzers[3,4]. The spacecraft maximum allowable concentration (SMAC[5]) of carbon monoxide is 10 $mg \cdot m^{-3}$, equivalent to 8.9 ppm in air at atmospheric pressure. This is generally at or below detection limit of electrochemical sensors and gas tubes. Non-dispersive infrared analyzers can measure CO at or below SMAC level with good precision, only at the cost of slow response time. SMAC levels for other species are very low (0.04 ppm for formaldehyde[5]), often well below detection limits of many existing sensors. Cross-sensitivity to interfering species such as water and carbon dioxide further aggravate the problem.

The goal for spacecraft gas monitoring is to have one small, easy-to-use device that can measure every contaminant found in the air, and make an accurate, real-time assessment over every possible range of concentration. Because no single instrument exists that can do all of these things, a variety of methods are used to make an assessment of the air quality. The quality of Space Shuttle air is measured by collecting contaminants in evacuated cylinders or on sorbent resin for post-flight ground-based analysis by gas chromatography (GC) and GC mass spectrometry[6]. Concentrations of major species such as nitrogen and oxygen are measured in flight, and some flights manifest a combustion products analyzer which measures carbon monoxide, hydrogen cyanide, hydrogen chloride, hydrogen fluoride, and carbonyl fluoride by electrochemical methods[7]. The International Space Station (ISS) has tighter requirements for air quality measurement because missions are longer. The ISS will have a Total Hydrocarbon Analyzer which will be used to identify leaks or spills of a wide variety of compounds using ion mobility spectrometry. The ISS will also have a Volatile Organic Analyzer, which will provide an in-flight assessment of targeted compounds using a gas chromatograph in conjunction with an ion mobility spectrometer. Even with this expensive and sophisticated set of instruments, a real-time assessment of many compounds, including formaldehyde, is not possible at this time. Small, reliable instruments that measure hard-to-detect compounds such as formaldehyde in real time in a spacecraft environment would be a helpful addition to the existing suite of instruments.

Reported herein is the design, performance testing, and field operation of a portable solid-state CO sensor based on diode laser pumped difference-frequency generation (DFG) at 4.6 μm. The sensor performs real-time measurement of CO in air at atmospheric pressure.

For CO levels between 0.1 and 10 ppm and a signal averaging time of 10 s, the measurement precision was 0.001 ppm. Absolute accuracy of the measurement was 0.6%, limited by the accuracy of the available CO reference. This is the first reported field application of a portable gas sensor based on diode-pumped mid-infrared DFG. The instrument measures 31 cm × 31 cm × 65 cm, consumes less than 50 W of electrical power, and uses no cryogenic or high-voltage components.

PRINCIPLES OF DFG

DFG[8] is a second-order nonlinear optical process in which a coherent light wave, "idler," is generated at the difference-frequency between two interacting light waves, "pump" and "signal":

$$\nu_i = \nu_p - \nu_s$$

The interaction generally occurs through nonlinear susceptibility of a dielectric crystal (Figure 1). Power in the idler wave is proportional to the product of pump power, signal power, and the length of interaction in the crystal:

$$P_i = C \cdot P_p \cdot P_s \cdot L \cdot h$$

Here C is the figure of merit of the nonlinear crystal, typically around 10^{-4} watt^{-1}cm^{-1}. The numerical function h quantifies the efficiency of focusing and overlap of pump and signal beams[8].

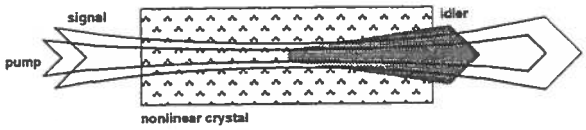

Figure 1. Schematic of the optical difference-frequency generation (DFG). Two focused Gaussian beams, pump and signal, produce a beat-note polarization wave in the nonlinear mixing crystal. The polarization wave generates an optical output beam, idler, at the difference frequency. Idler power is proportional to the product of pump and signal power, and the length of interaction.

DFG can provide frequency-tunable infrared light from two visible lasers. Recent feasibility studies have shown that this light is useful for spectroscopic detection of many important trace contaminants in ambient air (see Figure 2). Methane[9] and carbon monoxide[10], for example, were measured in natural air with 0.005 ppm precision in less than 60 seconds. Other tests have indicated that DFG has remote sensing capabilities.

An important element of a DFG source is the nonlinear mixing crystal. Its dispersion characteristics must satisfy the phase-matching condition to allow efficient interaction between pump and signal waves:

$$n_i \cdot \nu_i = n_p \cdot \nu_p - n_s \cdot \nu_s$$

The phase-matching condition is often difficult to meet in traditional birefringent[11] crystals. However, in periodically-poled lithium niobate (PPLN) – a new nonlinear optical material developed recently[12] – a similar *quasi*-phase-matching condition can be achieved through the manufacturing process:

$$n_i \cdot \nu_i = n_p \cdot \nu_p - n_s \cdot \nu_s - \frac{c}{\Lambda}$$

Here c is the speed of light, and Λ is the period of ferroelectric domain grating created in lithium niobate by application of a patterned strong electric field. The domain grating cancels out the otherwise destructive optical phase mismatch between the interacting beams. Quasi-phase-matching eliminates restrictions on pump and signal wavelengths and polarizations, allowing great flexibility in selection of laser sources and instrument design.

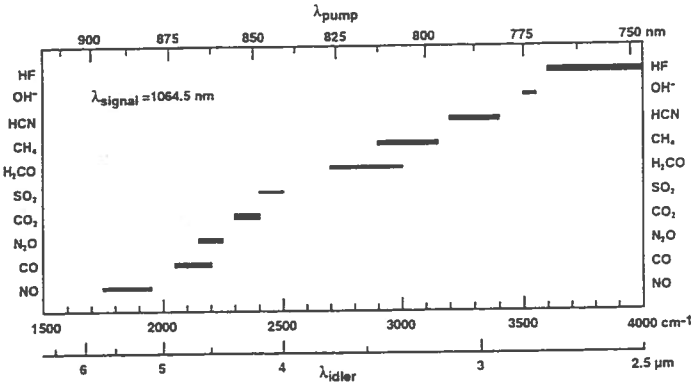

Figure 2. Mid-infrared (idler) wavelength coverage by difference-frequency mixing of a tunable diode pump laser and a 1064.5 nm Nd:YAG signal laser. Horizontal stripes indicate absorption wavelengths of several important trace air contaminants. Thickness of each stripe represents absorption strength.

INSTRUMENT DESCRIPTION

Figure 3 shows the instrument with cover removed. The 31 cm × 31 cm × 65 cm instrument case consists of two sections. Figure 4 shows a picture and a schematic diagram of the optical section, mounted on a 5 cm thick optical breadboard. Pump and signal lasers were used that are capable of reliable, low-noise, single-frequency operation over extended periods in an environment where vibration and changes in temperature and humidity are commonplace. The signal laser is a diode-pumped non-planar monolithic ring Nd:YAG laser with 750 mW output power at 1064.5 nm (Lightwave Electronics, Inc., Model 126). The pump laser is a 100 mW solitary GaAlAs diode laser at 865 nm (SDL, Inc., Model 5412), sealed in a metal can package together with a thermoelectric cooler, a monitor photodiode, and

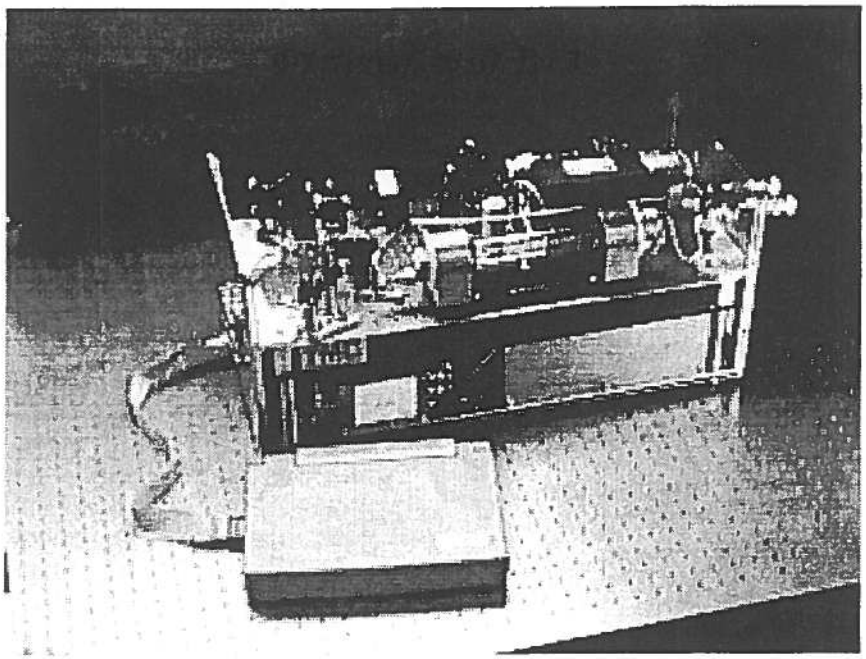

Figure 3. A photograph of the instrument with cover removed, showing optical components and electronics.

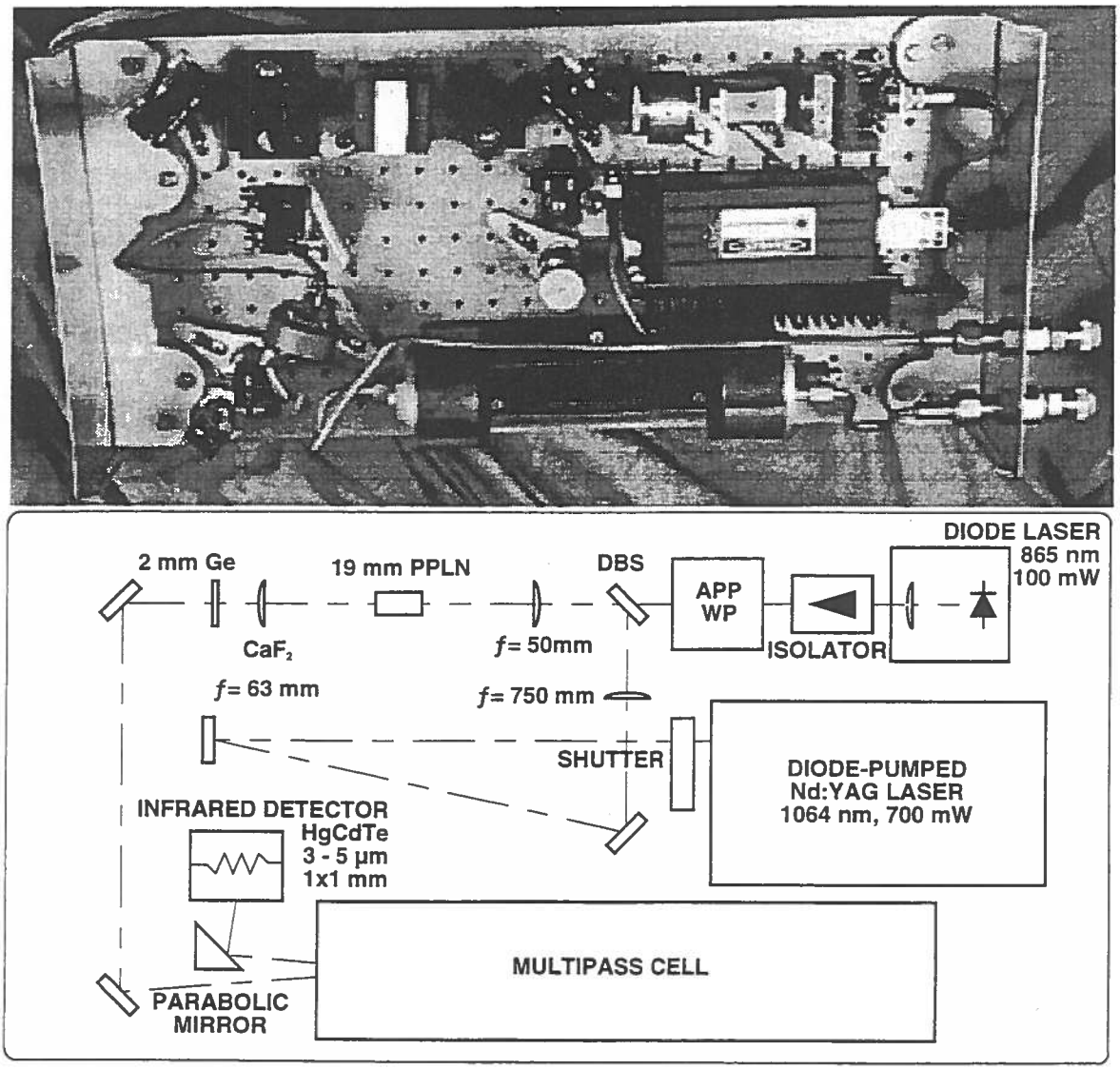

Figure 4. Diagram of the optical section. APP - anamorphic prism pair, WP - halfwave plate, DBS - dichroic beamsplitter.

a thermistor. Collimated output of the diode laser passes through a compact 40 dB optical isolator, a half-wave plate, and a 4× anamorphic prism pair, emerging as a vertically polarized beam 1.9 mm in diameter, spatially matched to the signal beam for efficient DFG. The pump and signal beams are combined by a dichroic beamsplitter and focused into an uncoated PPLN crystal measuring 19×11×0.5 mm (Crystal Technology, Inc.). The crystal has eight 1.3-mm wide strips with domain grating periods ranging from 22.4 μm to 23.1 μm in 0.1 μm steps. For difference-frequency mixing at 4.6 μm, the optimum period was found to be 22.9 μm at room temperature.

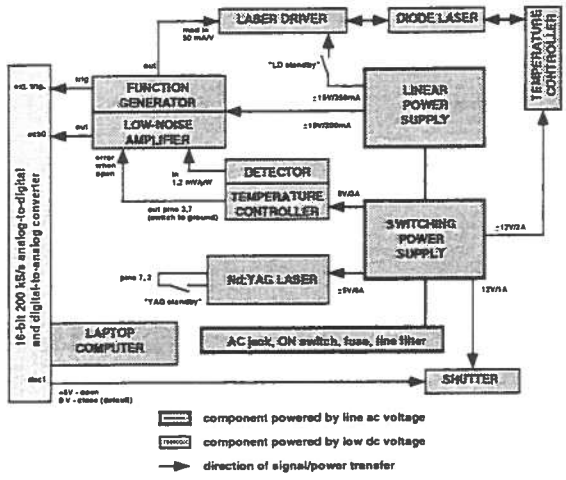

Figure 5. Diagram of the electronic section. A logic signal from the laptop computer drives the shutter circuit to periodically block the Nd:YAG beam for measurements of dark detector voltage.

With 70 mW pump power at 865 nm and 750 mW signal power at 1064.5 nm incident on the crystal, a typical idler power of 4.4 μW was measured. After collimation, the idler beam is separated from the pump and signal beams by a germanium filter.

The sensor employed a compact multipass cell (New Focus, Inc., Model 5611) aligned for an effective path length of 18.3 m. The cell increased absorption by CO in air to ~1%, so that the measured signal may substantially exceed detector noise and optical interference. An off-axis parabolic mirror at the output of the cell focused the idler beam onto a miniature infrared detector.

The instrument employed a mercury-cadmium-telluride detector with 1 mm^2 active area, cooled to –65°C by a three-stage Peltier cooler. The detector chip, along with the cooler and a thermistor, mounts in a sealed metal can package with an antireflection-coated sapphire window. Low-drift dc coupling of the detector allowed direct measurement of idler power necessary to determine percent optical absorption. Typical idler power measured after the multipass cell was 1.5 μW.

Detector output was digitized with a 12 bit, 100 kS/s analog-to-digital converter – part of a PCMCIA data acquisition card in a laptop computer (Figure 5). Digital output of the card controlled a small mechanical shutter to block the Nd:YAG beam for 3 seconds every minute, allowing the measurement of dark detector voltage.

A time trace of detector voltage averaged over 10 to 4000 sweeps, with dark voltage subtracted, constituted a measurement. For each measurement, the amplitude of CO absorption peak was extracted using nonlinear least-squares fitting[13]. The CO mole fraction in ppm was computed from the peak amplitude, displayed on the computer screen, and stored in a file along with a time stamp. Depending on the number of averages, the result could be updated every 1 to 80 seconds.

Direct absorption spectroscopy was chosen here because it offers adequate precision combined with the ease of signal processing and calibration. Alternatively, one can use wavelength-modulation spectroscopy[14], provided the modulation frequency falls within the gain bandwidth of the detector and the preamplifier. This method is attractive because of efficient reduction of noise bandwidth. However, it involves sophisticated signal processing and calibration.

INSTRUMENT TESTING AND CALIBRATION

The sensor response was calibrated by measuring optical absorption in an air sample with known CO content: 9.00 ± 0.05 ppm. Based on this absorption, another calibrated air sample with 1.030 ± 0.055 ppm CO was measured (Figure 6). Our result is 1.0559 ± 0.0008 ppm. The quantity 0.0008 ppm is the standard deviation of individual measurements, and is much smaller than the 0.6% initial accuracy of the calibration sample.

It was essential that the instrument be capable of long-term, unattended operation in the field environment. To measure the amount of long-term drift in alignment, output power, and idler frequency, the instrument was operated continuously for 2 weeks in the laboratory environment. Figure 7 shows an example of the CO concentration profile in room air recorded over 24 hours. Precision of this measurement was better than 0.005 ppm, despite the sometimes large swings in the magnitude of absorption signal. Temperature-dependent excursion of the operating frequency did not exceed 0.4 GHz. A quasi-periodic drift was observed in optical alignment coupled to changes in ambient temperature. It resulted in a typical 20% variation of the idler output power. Changes in operating frequency and output power were tracked by the data fitting algorithm and did not affect the measurements of concentration.

MEASUREMENTS OF CO IN CHAMBER AIR

NASA Johnson Space Center has recently completed the second, in a series of three chamber tests using a chamber outfitted for life support research and development (Figure 8). The tests are part of the Lunar-Mars Life Support Test Project (LMLSTP). In June of 1996, the chamber was outfitted with an air revitalization system, a water recovery system, necessary human accommodations, and four test subjects stayed in this closed life support system for 30

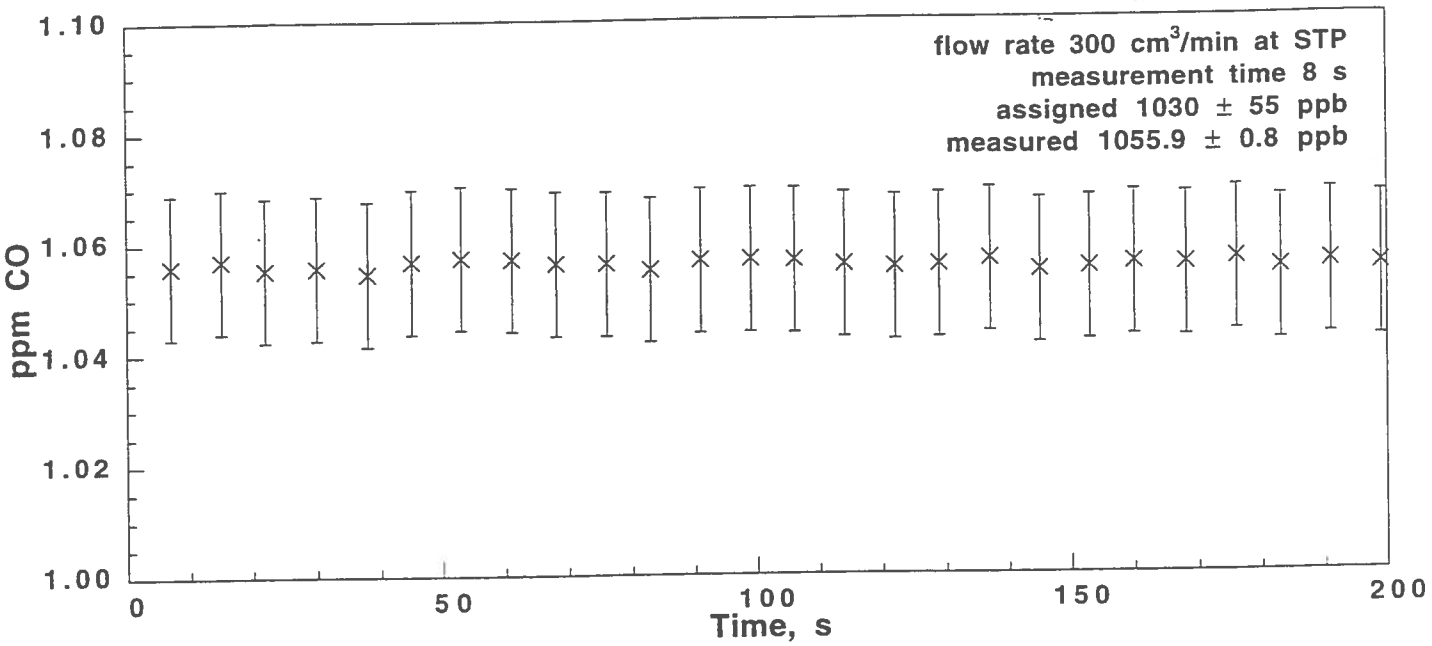

Figure 6. Measurement of air sample with factory-assigned CO content of 1030 ± 55 ppb. The value measured in the experiment is 1055.9 ± 0.8 ppb. Standard deviation of individual measurements (0.8 ppb) is well below the 0.6% initial uncertainty of sensor calibration, equivalent to 6 ppb. Error bars represent the root mean squared fit residuals, equivalent to 13 ppb CO

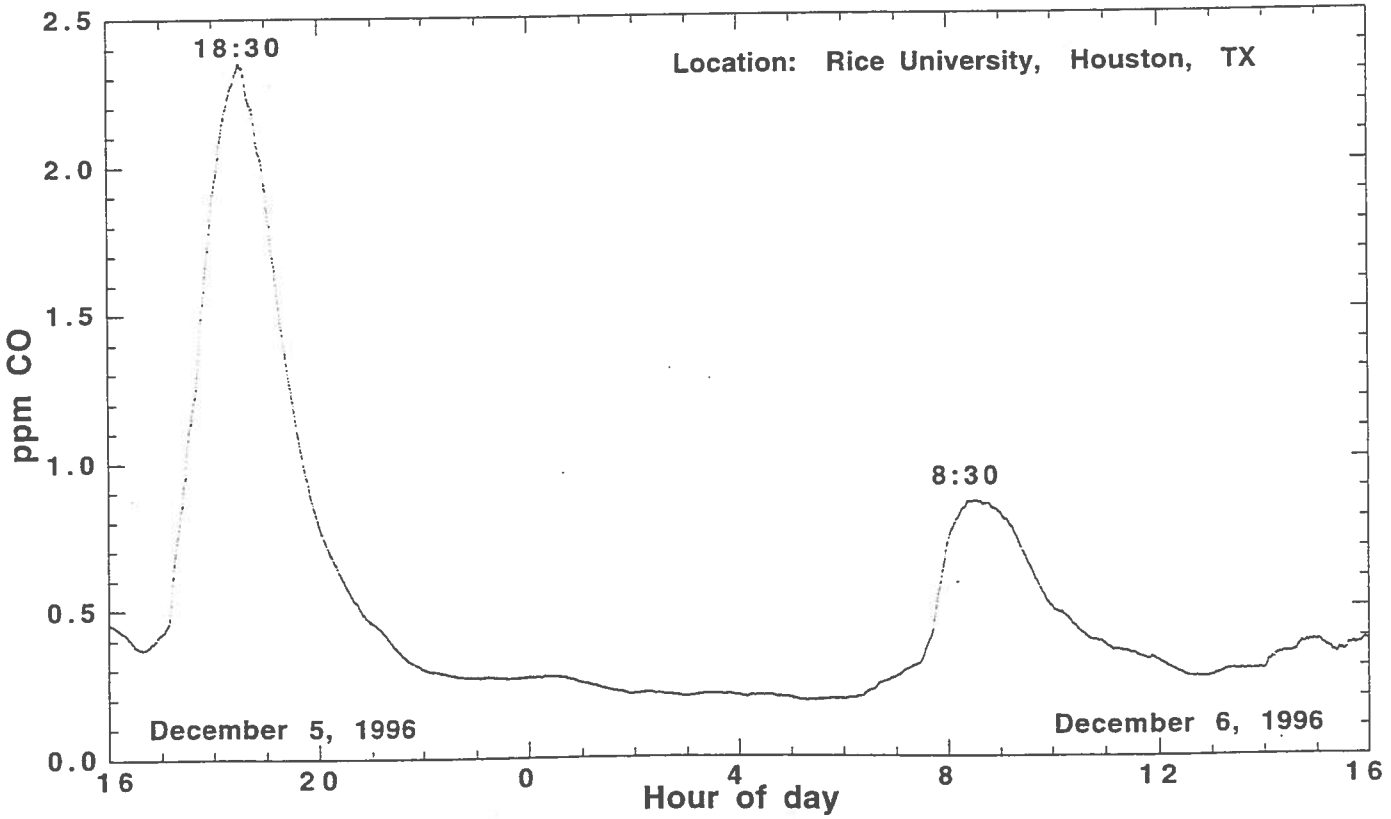

Figure 7. CO concentration in room air versus time, recorded at Rice University on December 5th/6th, 1996. The multipass cell was left open to allow convective flow of air. The peaks were observed during the evening and morning rush hours

days[15]. A detailed description of this test will be presented at a separate session of this ICES conference. After the June 1996 test, the chamber was modified so that the air revitalization system and the water recovery system had the same function and flow path as the life support system of the US portion of the ISS.

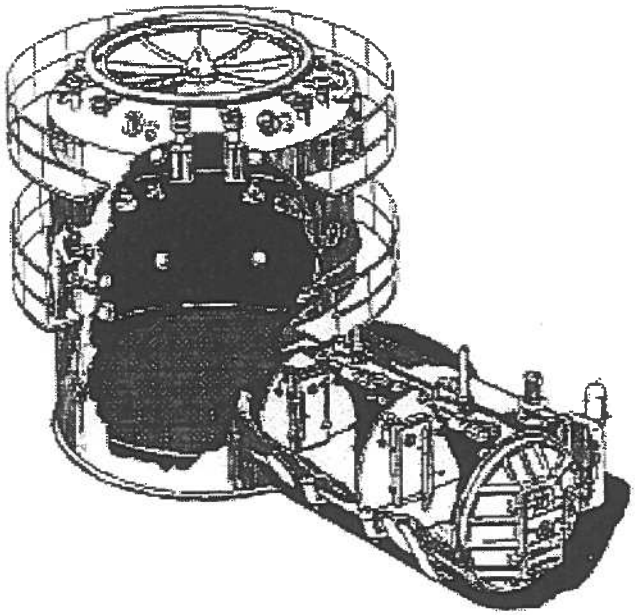

Figure 8. Schematic of the LMLSTP 20 ft test chamber.

In January 1997, four test subjects participated in a 60-day, closed chamber test. The CO sensor sampled chamber air for 16 days during this test. It operated outside the chamber and was connected to a sampling line with 0.02 $ft^3 \cdot min^{-1}$ air flow at atmospheric pressure. During the first three days, the sensor measured dehumidified air from the second level of the chamber, recording a 0.36 $ppm \cdot day^{-1}$ rise of CO concentration (Figure 9).

The instrument was then relocated to measure air sampled periodically from all levels in the chamber. The sensor operated at a location that was downstream from the sampling valve and upstream from the pump. The period of the sampling cycle was 34 minutes. The sampling valve closed for a short time during each cycle, leading to partial evacuation of the line. Figure 10 shows the resulting periodic decrease in the measured absorption signal. Measurements at the new location continued for 12 days, confirming the steady rise in CO concentration observed earlier.

Figure 11 shows the CO concentration profile recorded throughout the test. The average rate of increase in CO concentration was 0.41 $ppm \cdot day^{-1}$. Rapid exponential decrease in CO concentration beginning at 6:00 pm on January 24 is the result of catalytic oxidation in the Trace Contaminant Control System (TCCS). Based on the 8 $ft^3 \cdot min^{-1}$ throughput of the catalytic oxidizer, and the measured rate of exponential decay, an estimate of 9,300 ft^3 for the chamber volume was obtained. This estimate, along with the measured rate of increase in CO concentration, were used to compute the rate of CO production in the chamber (0.12 $g \cdot day^{-1}$).

CONCLUSION

A portable solid-state CO sensor based on diode-pumped difference-frequency generation at 4.6 μm was built and tested in laboratory and field environments. The sensor can measure CO in ambient air or in air flow with 0.001 ppm precision and 0.6% absolute accuracy in 10 seconds. Field test of the sensor consisted of two weeks of unattended operation outside a human rated chamber. The sensor recorded CO concentration profiles in chamber air during the LMLSTP Phase IIA test at NASA JSC.

It is proposed to modify the sensor for simultaneous detection of several trace air contaminants, including carbon monoxide, carbon dioxide, methane, and formaldehyde. This will require a tunable external-cavity diode laser operating at wavelengths between 816 nm and 865 nm. When used in conjunction with a Nd:YAG signal laser at 1064.5 nm, it will allow difference-frequency generation between 3.5 and 4.6 μm (see Figure 2). Based on the observed performance of the instrument in the field environment, it is expected to achieve real-time detection limits of better than 0.01 ppm for all of these species.

Diode-pumped DFG appears to be a good potential solution to the problem of ground-based trace gas detection. Further development of DFG gas sensors may lead to a variety of commercially viable, field-ready instruments. Several design modifications can reduce weight, size, power consumption, and cost of the DFG sensor. Output power of the pump and signal lasers can be reduced to 10 mW. This level of output power at wavelengths between 0.8 and 1.1 μm is available with low-cost, single-frequency monolithic diode lasers. They have low drive current threshold and high electrical-to-optical conversion efficiency at room temperature. The use of these lasers would greatly reduce electrical power consumption of the spectrometer.

The decrease in laser power would result in lower DFG output power, compromising detection sensitivity. To maintain the DFG output power in the range of a few microwatts, it is planned to use an adiabatically tapered periodically-segmented PPLN waveguide as a mixing element[16]. These devices yield DFG conversion efficiencies of 10 to 100 $\%\cdot W^{-1}$. Figure 12 shows a schematic diagram of the proposed open-path DFG gas sensor based on diode-pumped fiber-coupled PPLN waveguide. The use of fiber coupling is expected to reduce sensitivity to environment and vibration, decrease size and weight, and lower cost of the instrument[17].

Preliminary tests in the laboratory environment indicate that it is feasible to detect trace gases over 10 to 40 m open path in air using DFG. Open path detection

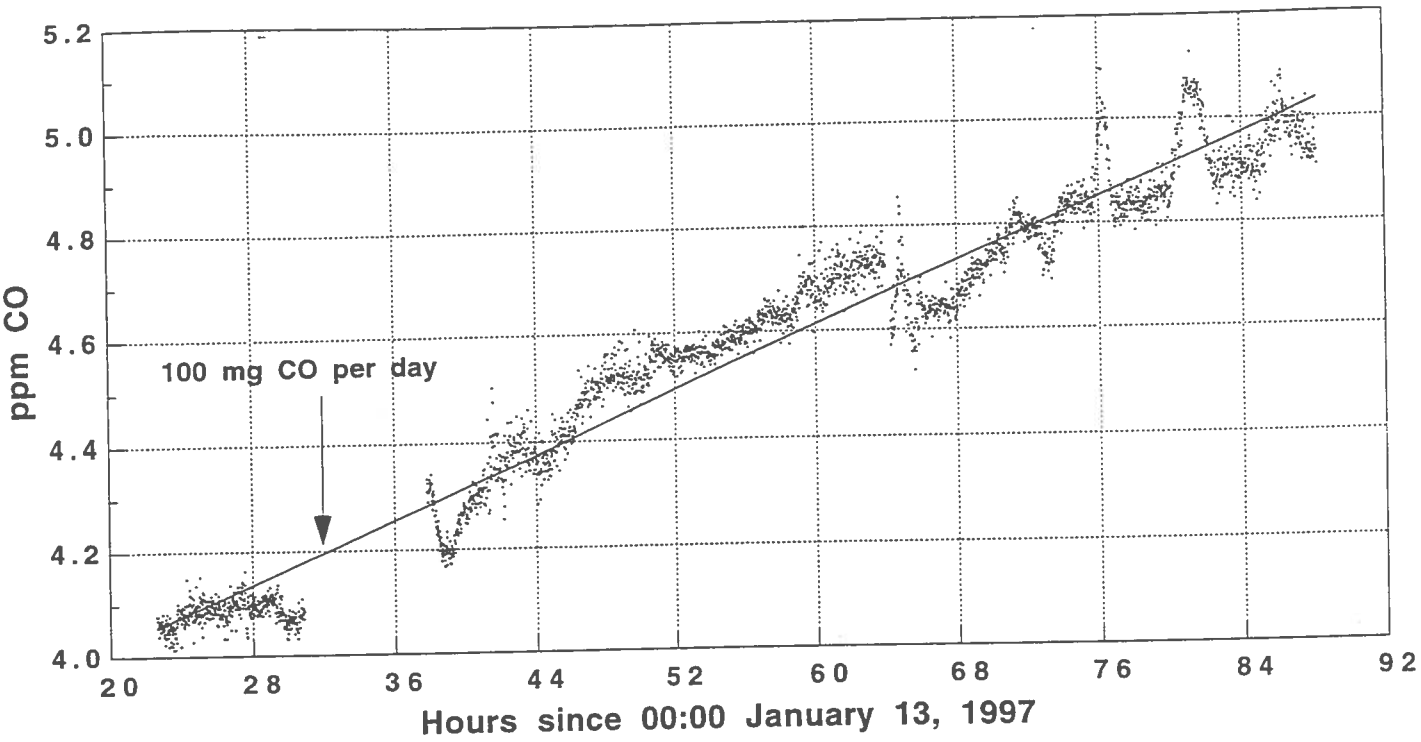

Figure 9. CO concentration profile in chamber air during the LMLSTP Phase IIA test at NASA JSC. The measurements were made in an air stream sampled from the 2nd level of the chamber.

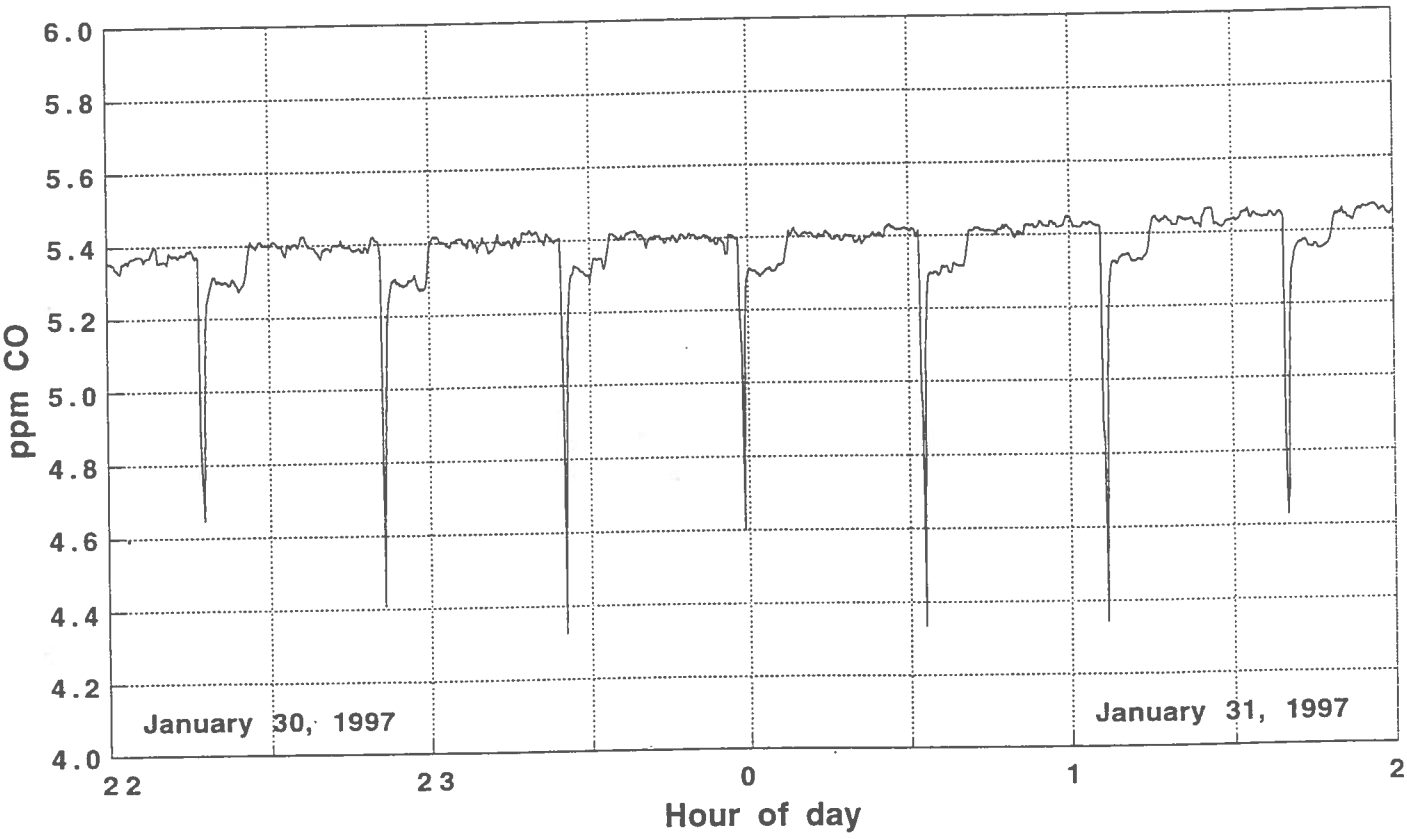

Figure 10. CO concentration in air which was periodically drawn from each level of the chamber. Periodic dips in concentration are an artifact ofpartial evacuation of the sampling line.

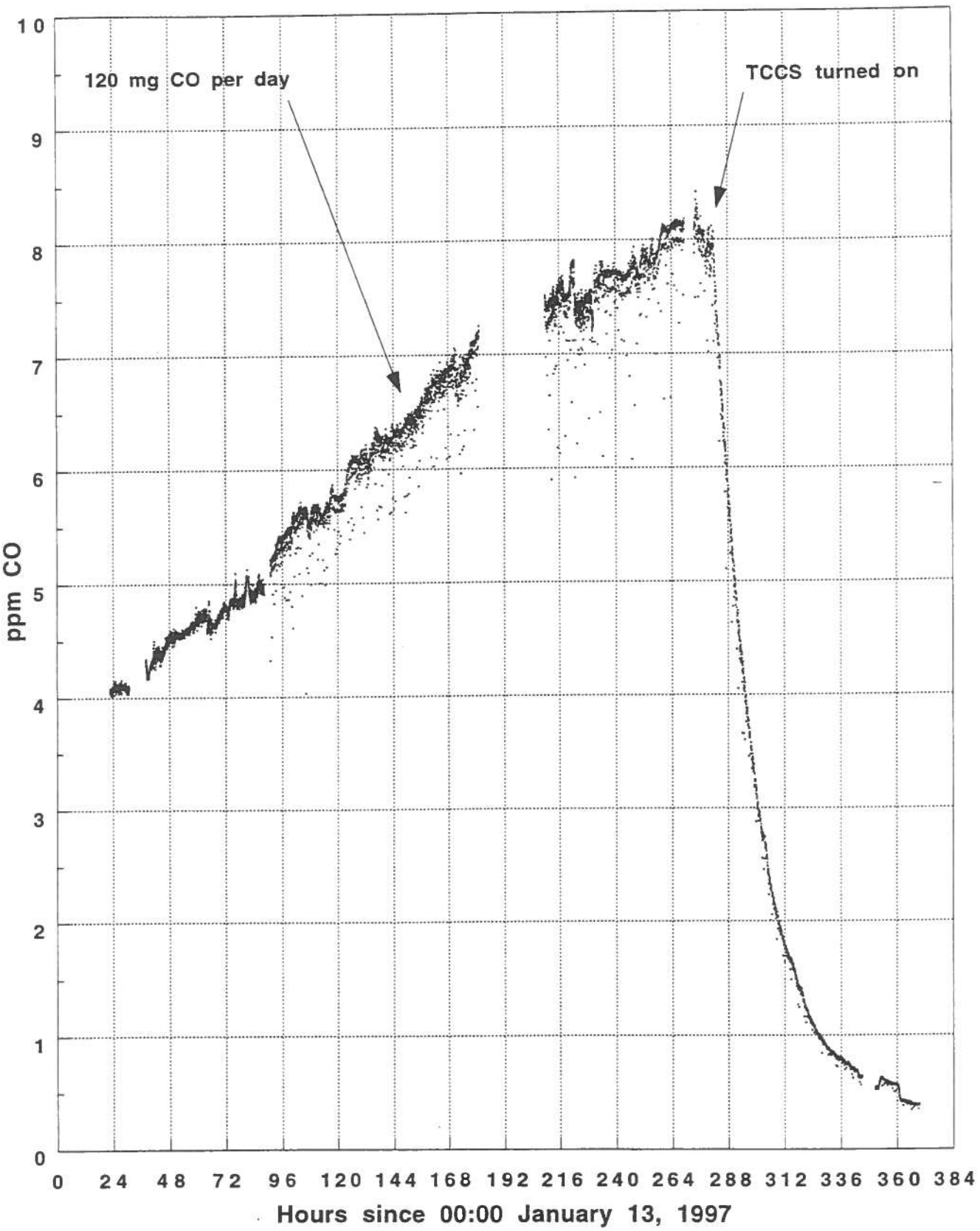

Figure 11. CO concentration profile in chamber air throughout the experiment. Rapid decrease in CO concentration beginning 6 pm January 24 is a result of catalytic oxidation in the Trace Contaminant Control System (TCCS).

has the advantage of high optical throughput, and the absence of optical interference due to scattering. We have performed measurements of CO over 20 m open path in air with the use of a 7 cm corner cube retro-reflector. The measurement precision was 0.0002 ppm, limited by detector noise.

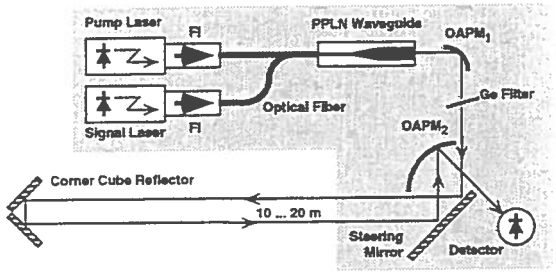

Figure 12. Schematic diagram of an open-path DFG gas sensor. It is proposed to use a PPLN waveguide pumped by low-power diode lasers. Fiber delivery of the pump and signal light into the waveguide ensures ruggedness and stability of alignment. Returned optical power is relatively independent of orientation of the corner cube reflector. FI - Faraday isolator; OAPM - off-axis parabolic mirror.

Diode-pumped DFG is a mature, although operationally complex, approach to trace gas detection. Another well developed approach is tunable diode laser absorption spectroscopy (TDLAS) in the near-infrared[18]. It uses a single monolithic diode laser operating in the region of spectroscopic overtone or combination-overtone absorption between 1.5 and 2.0 μm. These room-temperature lasers operate with 1 to 10 mW of output power, allowing shot-noise limited measurements of absorption[19] down to 10^{-7}. This is a factor of 100 better than that reported with the use of DFG. However, overall detection limit remains at a ppb (part in 10^9) level because the overtone absorption is a factor of 100 smaller than the fundamental absorption. Therefore DFG is perceived as a complementary method to TDLAS. DFG applies better to gas species whose overtone bands are either too weak, or interfered with by water, or inaccessible with near-infrared diode lasers. These include H_2CO, SO_2, CO, and NO.

ACKNOWLEDGMENT

The work performed by the Rice University authors was supported in part by NASA contract NAS-9-19553, Texas HECB grant 3604-036, and Welch Foundation grant C-0586.

REFERENCES

1. Motorola, Inc. "MGS1100 Carbon monoxide gas sensor," datasheet #MGS1100/D (1997).

2. B. H. Shah, R. J. Schmid, G. D. Franks: "Gas detector tube applications on space station Freedom," SAE Technical Paper Series #921150 (July 1992).

3. W. G. Fastie, A. H. Pfund, "Selective infrared gas analyzers," J. Opt. Soc. Am **37**, 762 (1947).

4. A. Galais, G. Fortunato, P. Chavel: "Gas concentration measurement by spectral correlation: rejection of interferent species," Appl. Opt. **24**, 2127 (1985).

5. J. T. James, H. W. Lane, S. L. Pool, D. E. Robbins: "Spacecraft maximum allowable concentrations for airborne contaminants," NASA Publication #JSC20584, p. 8 (February 1995).

6. J. James, T. Limero, H. Leano, J. Boyd, P. Covington: "Volatile organic contaminants found in the habitable environment of the Space Shuttle: STS-26 to STS-55," Aviation, Space, and Environmental Medicine (September, 1994).

7. T. Limero, S. Wilson, S. Perlot, J. James: "The role of environmental health system air quality monitors in Space Station contingency operations," SAE Technical Paper Series #921414 (July 1992).

8. T.-B. Chu, M. Broyer, "Intracavity CW difference-frequency generation by mixing three photons and using Gaussian laser beams," J. de Phys. **46**, 523 (1985).

9. K. P. Petrov, S. Waltman, E. J. Dlugokencky, M. A. Arbore, M. M. Fejer, F. K. Tittel, L. Hollberg, "Precise measurement of methane in air using diode-pumped 3.4 μm difference-frequency generation in PPLN," accepted for publication in Appl. Phys. B **64** (1997).

10. K. P. Petrov, L. Goldberg, W. K. Burns, R. F. Curl, F. K. Tittel, "Detection of CO in air by diode-pumped 4.6-μm difference-frequency generation in quasi-phase-matched $LiNbO_3$," Opt. Lett. **21**, 86 (1996).

11. G. Airoldi: "Nonlinear materials for tunable coherent light sources in the middle infra-red," Rivista del Nuovo Cimento **6**, 295 (1976).

12. E. J. Lim, H. M. Hertz, M. L. Bortz, M. M. Fejer, "Infrared radiation generated by quasi-phase-matched difference-frequency mixing in a periodically poled lithium niobate waveguide," Appl. Phys. Lett. **59**, 2207 (1991).

13. W. H. Press, B. P. Flannery, S. A. Teukolsky, W. T. Vetterling, *Numerical Recipes in Pascal,* Cambridge University Press p.572 (1989).

14. D. S. Bomse: "Dual-modulation laser line-locking scheme," Appl. Opt. **30**, 2922 (1991).

15. B. Laws, S. Foerg: "Early human testing of advanced life support systems, phase II and III," SAE Technical Paper Series #951491 (July 1995).

16. M. A. Arbore, M.-H. Chou, M. M. Fejer, "Difference frequency mixing in $LiNbO_3$ waveguides using an adiabatically tapered periodically-segmented coupling region," QELS '96 Technical Digest Series **10**, 42 (1996).

17. K. P. Petrov, L. Goldberg, R. F. Curl, F. K. Tittel: "Continuous-wave tunable 8.7-μm spectroscopic source pumped by fiber-coupled communications lasers," Opt. Lett. **21**, 1451 (1996).

18. M. G. Allen, W. J. Kessler, D. M. Sonnenfroh: "Room-temperature diode laser monitors for spacecraft air quality," SAE Technical Paper Series #97ES-78 (July 1997).

19. M. G. Allen, K. L. Carleton, S. J. Davis, W. J. Kessler, C. E. Otis, D. A. Palombo, D. M. Sonnenfroh: "Ultrasensitive dual-beam absorption and gain spectroscopy: applications for near-infrared and visible diode laser sensors," Appl. Opt. **34**, 3240 (1995).